applied sciences

MDPI

Article

Modeling of Cutting Force in the Turning of AISI 4340 Using Gaussian Process Regression Algorithm

Mahdi S. Alajmi [1,*] and Abdullah M. Almeshal [2]

[1] Department of Manufacturing Engineering Technology, College of Technological Studies, PAAET, P.O. Box 42325, Shuwaikh 70654, Kuwait
[2] Department of Electronic Engineering Technology, College of Technological Studies, PAAET, P.O. Box 42325, Shuwaikh 70654, Kuwait; am.almeshal@paaet.edu.kw
* Correspondence: ms.alajmi@paaet.edu.kw

Abstract: Machining process data can be utilized to predict cutting force and optimize process parameters. Cutting force is an essential parameter that has a significant impact on the metal turning process. In this study, a cutting force prediction model for turning AISI 4340 alloy steel was developed using Gaussian process regression (GPR), support vector machines (SVM), and artificial neural network (ANN) methods. The GPR simulations demonstrated a reliable prediction of surface roughness for the dry turning method with R^2 = 0.9843, MAPE = 5.12%, and RMSE = 1.86%. Performance comparisons between GPR, SVM, and ANN show that GPR is an effective method that can ensure high predictive accuracy of the cutting force in the turning of AISI 4340.

Keywords: artificial intelligence; machine learning; cutting forces; Gaussian process regression

Citation: Alajmi, M.S.; Almeshal, A.M. Modeling of Cutting Force in the Turning of AISI 4340 Using Gaussian Process Regression Algorithm. *Appl. Sci.* **2021**, *11*, 4055. https://doi.org/10.3390/app11094055

Academic Editors: Wilma Polini and José A. F. O. Correia

Received: 16 March 2021
Accepted: 27 April 2021
Published: 29 April 2021

1. Introduction

Turning is one of the most commonly employed manufacturing methods. With the growing number of applications for precision machining and machining of challenging materials, the modeling process is extremely necessary for evaluating the cutting force and the processing parameters to be optimized [1]. During the turning process, the surface finish is highly affected by parameters such as feed rate, cutting depth, cutting speed, and the radius of the tool nose [2]. For any machining operation, the selection of optimal cutting parameters is an important factor in increasing the quality and efficiency of the machined products, minimizing the costs of machining, and increasing production volume. The optimization of cutting parameters is also required to reduce cutting force during machining, since a high cutting force leads to several adverse effects, such as decreased tool life, high energy usage, increased surface roughness, bad finishing surfaces, etc. The cutting force plays a vital role in the metal cutting phase in the turning method, as it influences tool–workpiece deflection, vibration of machine tools, and finally the quality of the pieces. An accurate prediction of the cutting force during turning thus becomes an essential factor for process optimization and process characterization, and above all for improving machining efficiency [3]. However, defining the components of the cutting force is important for reducing energy usage in the process of metal cutting. Minimization of the cutting force directly controls the power consumption in the metal cutting industry, resulting in a greener, more ecological manufacturing operation by optimizing cutting parameters including cutting depth, feed rate, as well as cutting speed. The feed rate was identified as the primary cutting force parameter, whereas cutting speed is the prime parameter in reducing power consumption [4]. In addition, to acquire dimensional precision and machining device stability, the cutting force is necessary. In the area of interaction between the tools and the material, a cutting force occurs in all classic metal cutting processes, and it can be disintegrated by three orthogonal components [5]. In addition, it is exceedingly difficult to create an effective model because of the multiple interrelated parameters such as feed rate, cutting depth, cutting speed, nose radius, as well as cutting-edge angles, all of which affect the cutting force [6]. The cutting method is carried out while the tool is displaced, extracting a thin portion of the surface, which decreases the workpiece's diameter. The schematic in Figure 1 illustrates the normal turning mechanism forces; the parallel position of the cutting tool and speed of the spindle are shown as well.

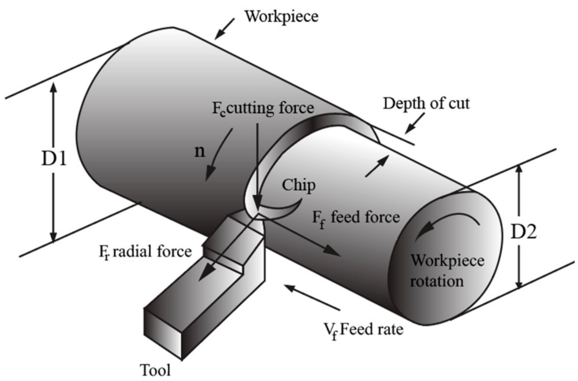

Figure 1. Turning process geometry.

Force equilibrium is identified as the connection between forces. The resultant cutting force is shown by Altintas [7], and it is produced from the feed force (F_f), the tangential cutting force (F_t), and the radial force (F_r) [7,8].

$$F_c = \sqrt{F_f + F_t + F_r} \tag{1}$$

F_f (feed force) is viewed in the direction of the thickness of the uncut chip and is influenced mainly by the feed rate. However, the feed force increases as the feed rate increases. F_t (tangential force) acts on the cutting speed (V) direction. F_r (feed force) is a radial force that moves the tool away from the workpiece, and it acts along the radial direction of the workpiece. According to the principle of equilibrium, the tool receives the same force in the same amplitude but in the opposite direction. The predicted cutting force F_c can then be defined as:

$$F_c = kv^{c_1} f^{c_2} d^{c_3} \tag{2}$$

where k, c_1, c_2, and c_3 are model parameters.

In the last few decades, there has been diverse modeling processes focused on artificial neural networks and fuzzy sets; most researchers use these tools to forecast various machining processing parameters including tool wear, cutting force, and machined-piece surface roughness. It is very important to model and forecast cutting force in the turning mechanism, since it is directly connected to the consistency of the processed surface, self-excited vibrations, tool wear, etc. To estimate the strength needs for machinery tools, an understanding of cutting force is crucial. An awareness of cutting force is necessary for the appropriate selection of operative conditions and machine equipment because equipment and tools contribute to an effective machining operation. In addition, the monitoring of the cutting force is used for detecting breakage and tool wear. The cutting method is highly complex, and so it is difficult to precisely model the cutting force due to the many highly interconnected variables that influence those forces.

Several investigations to model the cutting force in the turning process exist in the literature. Hanief et al. [8] established a model to examine the impact of cutting parameters on cutting force using a high-speed steel (HSS) instrument during the red brass turning process (C23000). Multiple regression as well as artificial neural network (ANN) techniques were used. The ANN model was considered to be more precise compared to the regression model. For turning mechanisms, a mechanistic cutting force model was introduced by Zhang and Guo [9]. This model defines the cutting region distribution and measures the immediate efficient tool angles, cutting force, cutting parameters, force intensity, and their distribution. The findings suggest that the force and the force intensity distributions on the instrument edge provide important information for the estimation of the turning force/power and a possible additional estimation of tool wear existence. Fodor et al. [10] demonstrated how Gaussian white noise stochastic processes could be used to characterize the cutting force in material-eliminating mechanisms. This method contributes to stochastic differential equations that are mathematically dynamic problems. The findings showed that the variability of the calculated force signal typically stands at about 4–9% of the average value, which is greater than the noise emerging from the measuring device. Zerti et al. [11] applied the ANN and response surface methodology (RSM) approach for modeling output parameters in the dry hard turning process of AISI 420 (martensitic stainless steel) processed at 59HRC. The findings showed that cutting depth has a strong effect on the cutting force, the removal capability, and the material removal rate (MRR). The association between the essential parameters (nose radius, feed rate, and cutting speed) and their effect on the turning force components was investigated by Tzotzis et al. [12]. The distinction between the resultant values of the cutting force factors and the simulations revealed an improvement in the association of over 89%. The values obtained from the mathematical model were also based on the confirmed appropriateness in line with the corresponding finite element model values. As an operation of cutting parameters, Patel and Gandhi [13] established an analytical trend for cutting forces. The force model is expanded with an empirical method focused on the Waldorf principle in ideal cutting conditions, taking into account the progression of flank wear. The findings demonstrated the efficiency of analytical models established for the estimation of cutting force. Sharma et al. [14] suggested a prediction model for the cutting force for hard turning operations. In this work, the ANOVA research showed how each machining parameter contributes to the estimation and analysis of the cutting force. The established fuzzy model was considered to be satisfactory and better than the regression model for estimation purposes. The association between the cutting force coefficients and the cutting power was analyzed by Qiu [15]. A linear relationship between the MRR and spindle strength was developed in the cutting power model. The findings demonstrate that the cutting force coefficients derived through the calculation of the cutting power are in agreement with that determined by the dynamometer.

Significant attention has recently been paid to the establishment of optimization as well as predictive models to understand the impact of machining parameters on cutting force, where artificial intelligence techniques are used as an alternative to standard approaches such as milling, drilling and grinding. A hybrid optimization algorithm based on ANN and a genetics algorithm (GA) was utilized to model the surface roughness and cutting force in a milling machine in [16]. Chen et al. presented a hybrid algorithm based on adaptive particle swarm optimization, a least squares algorithm, and a support vector machine (APSO-LS-SVM) to monitor and predict tool wear in the drilling process as reported in [17]. In addition, the monitoring of tool condition in the grinding process based on a support vector machine (SVM) and a genetics algorithm was reported in [18]. Furthermore, ANN was utilized for surface quality control in machining systems based on multisensor data fusion [19]. Similarly in [20], the ANN model was used to monitor surface quality in a taper turning CNC machine.

In this work, we present the use of Gaussian process regression (GPR) in estimating the cutting force in the turning process. As far as we know, the literature has insufficient detail regarding the usage of GPR for estimating the cutting force in the turning process. Furthermore, the technique of GPR has not been examined before for modeling and predicting cutting force values in a turning process. The aim of the current study is to assess the precision of GPR in the modeling of experimental results for turning AISI 4340 alloy steel. The suggested GPR technique is discussed in the following section. The findings of the simulation provide the expected outcomes and demonstrate the predictive precision of GPR in contrast with SVM and ANN methods

2. Design of Experiment and Data

The data used in this research were retrieved from the experiment reported in [21]. We applied the machine learning algorithm to predict the data and compared the findings with the actual experimental results reported by the authors in [21]. The experiment was conducted using a Maxturn++ (MTAB, Tamilnadu, India) CNC lathe machine with a swing of 410 mm over the bed, a standard turning diameter of 200 mm, a weight of 2500 kg, and a maximum turning length of 360 mm. The rapid feed rate was 30 m/min, and the 7 KW spindle motor power has a speed range of 50–6000 rpm. The X-axis was 140 mm, and the Z-axis was 380 mm in length.

The cutting forces were measured using a Kistler dynamometer (Kistler Instrument Corporation, Novi, MI, USA), and the surface roughness tester SJ-201P by Mitutoyo (Mitutoyo, Aurora, IL, USA) was used to measure surface roughness. The range of input parameters is shown in Table 1, and the experimental data results are reported in Table 2. The experimental results in Table 2 were obtained from the conventional experimental procedure and are used in this research to train the GPR algorithm to predict the cutting force. In the next section, the methodology of the GPR, ANN, and SVM is presented to predict the cutting force of the turning process.

Table 1. Input parameters range values.

Parameter	Range
Cutting speed (m/min)	75, 90
Feed rate (mm/rev)	0.04, 0.06, 0.08, 0.1, 0.12
Depth of cut (mm)	0.5, 1, 1.5
Tool nose radius (mm)	0.4, 0.8
Air pressure (bar)	5
Fluid flow rate (mL/h)	140

Table 2. Experimental results [21].

No.	Cutting Speed (m/min)	Nose Radius (mm)	Feed Rate (mm/rev)	Depth of Cut (mm)	Surface Roughness (μm)	Average Cutting Force (N)
1	75	0.8	0.04	1.5	1.01	22.45
2	75	0.8	0.04	1	1.06	15.52
3	75	0.8	0.04	0.5	1.26	7.67
4	75	0.8	0.06	1.5	1.24	33.21
5	75	0.8	0.06	1	1.32	23.15
6	75	0.8	0.06	0.5	1.35	11.7
7	75	0.8	0.08	1.5	1.42	39.85
8	75	0.8	0.08	1	1.5	28.07
9	75	0.8	0.08	0.5	1.61	13.58
10	75	0.8	0.1	1.5	1.6	45.42
11	75	0.8	0.1	1	1.64	32.82
12	75	0.8	0.1	0.5	1.75	16.94
13	75	0.8	0.12	1.5	1.7	52.26
14	75	0.8	0.12	1	1.78	37.25
15	75	0.8	0.12	0.5	1.88	19.15
16	90	0.8	0.04	1.5	1.29	20.72
17	90	0.8	0.04	1	1.37	14.14
18	90	0.8	0.04	0.5	1.4	7.81
19	90	0.8	0.06	1.5	1.41	31.38
20	90	0.8	0.06	1	1.5	21.45
21	90	0.8	0.06	0.5	1.56	10.66
22	90	0.8	0.08	1.5	1.67	39.14
23	90	0.8	0.08	1	1.72	28.21

Table 2. *Cont.*

No.	Cutting Speed (m/min)	Nose Radius (mm)	Feed Rate (mm/rev)	Depth of Cut (mm)	Surface Roughness (μm)	Average Cutting Force (N)
24	90	0.8	0.08	0.5	1.8	14.74
25	90	0.8	0.1	1.5	1.78	44.22
26	90	0.8	0.1	1	1.82	31.56
27	90	0.8	0.1	0.5	1.93	16.52
28	90	0.8	0.12	1.5	1.93	50.61
29	90	0.8	0.12	1	2.02	36.72
30	90	0.8	0.12	0.5	2.16	19.46
31	75	0.4	0.04	1.5	1.09	22.56
32	75	0.4	0.04	1	1.21	15.16
33	75	0.4	0.04	0.5	1.5	6.62
34	75	0.4	0.06	1.5	1.12	31.44
35	75	0.4	0.06	1	1.32	21.19
36	75	0.4	0.06	0.5	1.64	9.71
37	75	0.4	0.08	1.5	1.15	38.82
38	75	0.4	0.08	1	1.4	27.5
39	75	0.4	0.08	0.5	1.93	12.64
40	75	0.4	0.1	1.5	1.28	45.55
41	75	0.4	0.1	1	1.56	31.73
42	75	0.4	0.1	0.5	2.08	15.48
43	75	0.4	0.12	1.5	1.47	52.8
44	75	0.4	0.12	1	1.82	37.14
45	75	0.4	0.12	0.5	2.32	17.57
46	90	0.4	0.04	1.5	2.07	22.78
47	90	0.4	0.04	1	1.42	14.56
48	90	0.4	0.04	0.5	1.75	6.87
49	90	0.4	0.06	1.5	2.22	30.81
50	90	0.4	0.06	1	1.5	20.5
51	90	0.4	0.06	0.5	1.88	10.2
52	90	0.4	0.08	1.5	2.31	39.8
53	90	0.4	0.08	1	1.67	27.48
54	90	0.4	0.08	0.5	2.15	13.44
55	90	0.4	0.1	1.5	2.52	46.15
56	90	0.4	0.1	1	1.82	31.88
57	90	0.4	0.1	0.5	2.28	16.25
58	90	0.4	0.12	1.5	2.9	51.12
59	90	0.4	0.12	1	2.07	36.57
60	90	0.4	0.12	0.5	2.52	18.7

3. Methodology

In this section, an overview of the GPR, ANN, and SVM algorithms is presented to predict the cutting force in a turning process using cutting speed, nose diameter, feed rate, surface roughness, and depth of cut parameters as inputs. This research presents the GPR as the main algorithm for predicting cutting force values, and the results are compared with ANN and SVM prediction performances to assess the GPR's performance.

3.1. Gaussian Process Regression (GPR)

Gaussian process regression is a machine learning method based on Bayesian theory [22]. GPR is feasible for small size datasets, nonlinear, complex, and high dimensional regression problems [23,24]. Unlike linear regression, GPR is a collection of random variables that have a joint Gaussian distribution with a mean and covariance function.

For a training dataset with n training data points with inputs and target variables $\{x_i, y_i\}$ and $i = 1, 2, \ldots, n$ respectively, the model is defined as:

$$y_i = f(x_i) + \epsilon_i \tag{3}$$

where $f(x_i)$ is the learning function and ϵ_i is Gaussian noise with zero mean and variance σ_n^2. The target variables y_i are described with Gaussian distribution as:

$$y \sim \mathcal{N}\left(0, K(X,X) + \sigma_n^2 I\right) \tag{4}$$

with $K(X,X)$ denoting the covariance matrix. In this research, a Gaussian kernel is used as the covariance function and is written as:

$$k\left(x_p, x_q\right) = \sigma_s^2 \mathrm{e}^{\left(-0.5\left(x_p - x_q\right)^T W\left(x_p - x_q\right)\right)} \tag{5}$$

where the signal variance corresponds to σ_s^2 and W is the width of the Gaussian kernel. For a point x^*, the joint Gaussian distribution of the observed target values and the predicted values is given by:

$$\begin{bmatrix} y \\ f(x^*) \end{bmatrix} \sim \mathcal{N}\left(0, \begin{bmatrix} K(X,X) + \sigma_n^2 I & k(X,x^*) \\ k(x^*,X) & k(x^* x^*) \end{bmatrix}\right) \tag{6}$$

and yields to the predicted mean value of the learning function $f(x^*)$ with the variance $V(x^*)$ are given as:

$$f(x^*) = k^{*T}\left(K + \sigma_n^2 I\right)^{-1} y = k^{*T}\alpha \tag{7}$$

$$V(x^*) = k(x^*, x^*) - k^{*T}\left(K + \sigma_n^2 I\right)^{-1} k^* \tag{8}$$

where α, $k^* = k(X,x^*)$ and $K = K(X,X)$ present the prediction vector. The remaining parameters $\theta = \left[\sigma_n^2, \sigma_f^2, W\right]$ are the hyperparameters of the Gaussian process that can be optimized using standard optimization algorithms.

3.2. *Artificial Neural Networks (ANN)*

Artificial neural networks are inspired by the human brain's biological structure. A simple ANN consists of an input layer, a hidden layer, and an output layer [25]. It mimics the behavior of the human brain to solve complex data-driven problems. The neural units are fed with input data that are processed via hidden layers to produce the desired output. ANNs are utilized by various studies across many fields with proven results in both supervised learning and unsupervised learning problems such as classification and regression real-time problem. In a simple ANN model, some inputs with corresponding multiple weight values are added with bias values along with a threshold that is defined by the activation functions to predict the output.

Depending on the problem, whether a classification or a regression problem, the activation function for ANN that makes a decision is defined by the rectified linear unit (ReLu) function, the hyperbolic tangent (Tanh) function, or the Sigmoid function. The ReLu function ensures the output is not less than zero, $f(a) = \max(0, a)$, while the Tanh function finds the hyperbolic output. Here, $f(a) = \tanh(a)$, and the Sigmoid function is defined as $f(a) = \frac{1}{\left(1+e^{-1*z}\right)}$.

In this work, a fully connected ANN with two layers and 15 neurons at each layer is utilized to predict the cutting force value as an output.

3.3. *Support Vector Machine*

The SVM is one of the most popular supervised learning-based machine learning algorithms that solves classification as well as regression problems [25]. The main objective of the SVM is to find the best hyperplane for the given data points in an N-dimension space where N is the number of features. To draw a boundary between the data points of two classes, there are many possible hyperplanes that separate the two classes. The objective is to find a hyperplane that takes the maximum distance between the two classes and provides support so that the predated data points are classified with high accuracy.

In regression problems, the SVM fits the data points into a straight line with y = wx + b, which is referred to as a hyperplane, and the data points closest to either side of the hyperplane define the support vector's boundary line. However, the difference between the linear regression and the SVM is that the SVM fits the best line within the minimum distance between the hyperplane and the boundary line that can satisfy the condition—a < y − wx + b < a.

3.4. Performance Metrics

To assess the prediction performance of the methods, various statistical performance indicators are utilized such as the root mean square (*RMSE*), the standard deviation (STD), the mean absolute error (*MAE*), the coefficient of variation of root mean square error (*CVRMSE*), and the mean absolute percentage error (*MAPE*). In addition, the coefficient of determination R^2 provides a measure of how closely the prediction matches the actual values. These measures are defined as:

$$MAE = \frac{1}{n}\sum_{i=1}^{n}|y_i - \hat{y}_i| \tag{9}$$

$$MAPE = \frac{1}{n}\sum_{i=1}^{n}\left|\frac{\hat{y}_i - y_i}{y_i}\right| \times 100\% \tag{10}$$

$$R^2 = 1 - \frac{\sum_{i=1}^{n}(y_i - \hat{y}_i)^2}{\sum_{i=1}^{n}(y_i - \breve{y})^2} \tag{11}$$

$$RMSE = \frac{\sqrt{\sum_{i=1}^{n}(\hat{y}_i - y_i)^2}}{n} \tag{12}$$

$$CVRMSE = \frac{\sqrt{\sum_{i=1}^{n}(\hat{y}_i - y_i)^2}}{\breve{y}} \tag{13}$$

4. Results and Discussion

The GPR algorithm was executed in the MATLAB software (Mathworks, Natick, MA, USA) package to model the cutting force for turning AISI 4340 alloy steel with reference to experimental data reported in [21]. The actual data of the turning process of AISI 4340 compared to GPR, SVM, and ANN are presented in Table 3, showing 60 trials of each process to evaluate every combination of input parameters of depth of cut, cutting speed and feed rate, while the output response variable is the resultant force. The resultant forces changed within the individual trials due to the change of input parameters. Table 2 provides the statistical performance indicators of each method in terms of the *MAPE*, *RMSE*, *MAE*, and R^2 values. It is noted that GPR achieved the best accuracy in predicting the surface roughness values with RMSE of 1.86% and a high coefficient of determination value of R^2 = 0.98. The high value of R^2 clearly indicates that the predicted values closely match the actual experimental values of the surface cutting force, and the superior performance of the GPR is evident, due to the algorithm's superiority in exploring the search space and avoiding the local optima trap. The SVM provides the second-best prediction values with an *RMSE* of 3.07% and an R^2 of 0.97. This can be addressed to the gradient ensemble in combining different weak learners into a meta learner that provides the best prediction at each step. The ANN resulted in a relatively comparable performance with the SVM method in terms of the coefficient of determination with R^2 = 0.947. However, it has a slightly higher RMSE value of 3.46%, which is higher than the SVM algorithm by 0.27%.

Table 3. Comparison results of $F_c(N)$ for actual cutting forces, GPR, SVM, and ANN measured in kgf.

Data	Actual	GPR	SVM	ANN
1	22.45	25.0529771	22.91932087	24.21418804
2	15.52	15.828919	15.70293258	16.36564709
3	7.67	8.53333862	9.021956651	11.80074896
4	33.21	31.2012136	29.84178436	30.80456182
5	23.15	22.089346	21.3083986	21.40719968
6	11.7	11.4624395	12.66595967	10.73101918
7	39.85	39.5438043	33.74027778	39.53554623
8	28.07	28.0919717	26.50360215	28.75123913
9	13.58	14.5048494	11.73586611	14.25102381
10	45.42	46.431982	43.07109445	48.09695993
11	32.82	32.7805683	30.06625841	34.06079817
12	16.94	17.0203249	17.81597692	18.50273521
13	52.26	48.0807784	44.70294639	43.76071549
14	37.25	35.2788251	33.20572228	33.3668117
15	19.15	22.0473817	19.52311889	22.06577018
16	20.72	24.4285024	23.10524016	23.62156834
17	14.14	15.4355581	14.98431965	14.48325075
18	7.81	7.64684253	8.267628928	10.59143006
19	31.38	31.093137	30.76954699	29.57011778
20	21.45	21.4600877	20.57752531	19.80906493
21	10.66	11.2552626	11.27866576	11.46983893
22	39.14	38.3636644	38.25223323	39.22916097
23	28.21	27.3290981	26.73283079	28.15712769
24	14.74	14.0246408	12.56687461	14.21767067
25	44.22	45.1105649	42.19021155	46.43950914
26	31.56	32.4718376	31.91753592	34.5871173
27	16.52	19.1383276	16.9789595	20.95898138
28	50.61	47.6740405	42.54547675	43.78563235
29	36.72	35.8412734	32.38550878	36.04813972
30	19.46	20.2009669	19.06031562	19.33064084
31	22.56	25.3868501	23.76891638	26.40105304
32	15.16	16.3210017	15.41406766	17.33112468
33	6.62	7.18989911	8.171158719	10.40235966
34	31.44	30.4522226	29.76639077	29.87597985
35	21.19	21.1824123	21.3083986	21.01016136
36	9.71	10.0628118	11.66739689	9.439559173
37	38.82	37.6892054	38.5617505	36.8477515
38	27.5	26.8557951	27.15839851	27.05053072
39	12.64	12.9071058	12.72158606	14.11821133
40	45.55	44.8192269	41.87706371	43.77448873
41	31.73	33.2514357	31.3627139	34.57937336
42	15.48	15.6544623	16.79119579	16.61167088
43	52.8	48.2831198	42.54547675	45.93563199
44	37.14	36.1242241	33.14722804	35.70802991
45	17.57	20.5531402	19.56785604	19.7815983
46	22.78	25.6403883	30.1046451	26.20319935
47	14.56	15.0127202	14.91622958	16.29281976
48	6.87	7.22640958	8.584091261	10.83896043
49	30.81	30.5587044	30.42904924	29.27838599
50	20.5	20.5362971	20.45468095	19.39878201
51	10.2	10.2576783	11.61973357	10.02784569
52	39.8	37.5289976	38.23346895	35.38788695
53	27.48	25.9991416	26.9948135	25.16690996
54	13.44	13.6138121	12.72158606	14.09786533
55	46.15	44.0283559	41.47029172	40.52117368
56	31.88	31.4100057	30.42133004	31.34682703
57	16.25	16.6632828	17.21730724	17.51374508
58	51.12	43.8205786	43.37659946	36.54195755
59	36.57	35.3314071	32.69978926	33.66115622
60	18.7	21.1436962	18.82467991	21.13694601

The computational cost of the methods was measured in terms of the time to train the algorithm to predict the data. The GPR was trained on the input dataset within 0.3507 s, while the ANN and SVM were trained within 1.3395 s and 0.88296 s, respectively. GPR is superior in terms of the amount of training time, and it produces the highest prediction accuracy in terms of the performance metrics in Table 4.

Table 4. Performance measure for the GPR, SVM, and ANN for turning process for AISI 4340.

Indicator	GPR	SVM	ANN
STD	11.8659845	10.8311621	10.9700107
MAPE	5.12881818	7.91289907	10.8512889
MAE	1.2790129	2.05869621	2.3533598
MSE	3.46918946	9.43121873	11.1943294
RMSE	1.86257603	3.07102894	3.34579279
CVRMSE	15.6967677	28.353642	30.4994487
R^2	0.9843	0.9711	0.9475

Figure 2 illustrates a graphical comparison between the actual cutting force values and the values predicted by the GPR, SVM and ANN methods. The superior prediction performance of the GPR can be clearly noted by the close match of each data point on the graph with the actual value of the surface roughness. Figure 3 shows the trend line between the actual versus the predicted values of each prediction algorithm in order to provide the coefficient of determination values R^2.

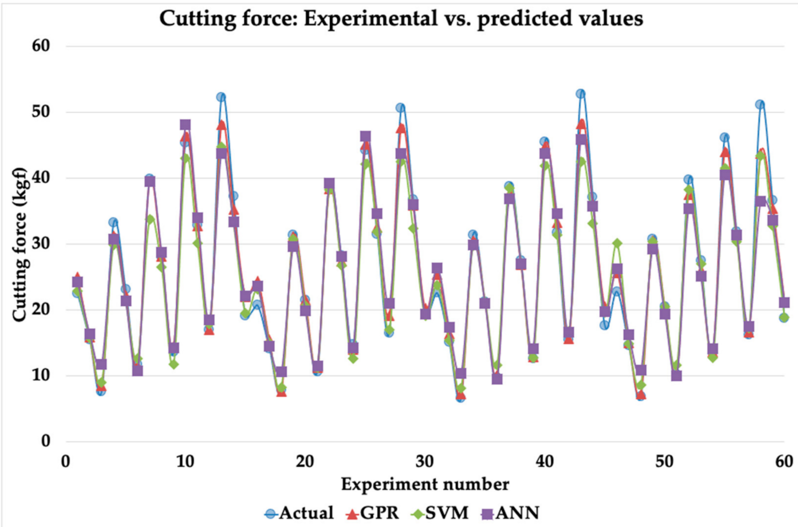

Figure 2. Actual cutting force values in comparison with predictions by GPR, SVM, and ANN methods.

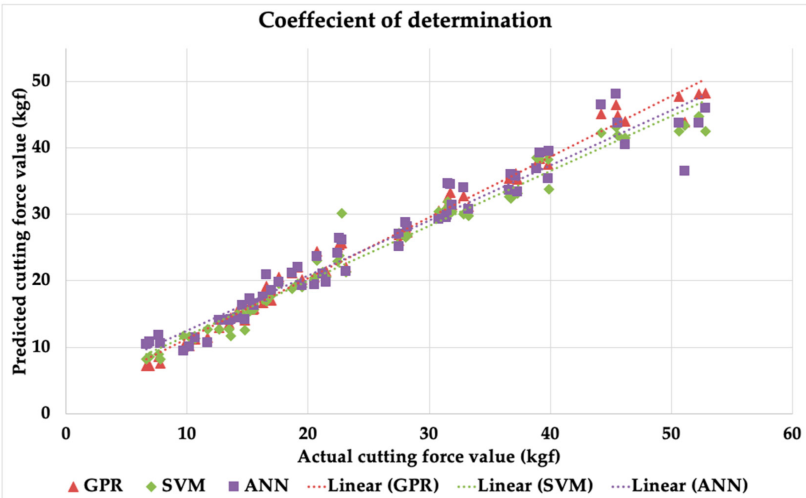

Figure 3. Actual values of the cutting force in comparison with values predicted by GPR, SVM, and ANN and coefficient of determination trend lines.

With the results obtained in this section, it is evident that GPR yields promising results in the field of predicting and modeling the cutting forces in a turning process. One limitation of the GPR algorithm is that it is only feasible for datasets of a few thousands [26] due to the computation of matrix inversions, which is highly computation-intensive for large datasets. However, this limitation may not be a barrier in applying the GPR to predict the parameters of a turning process due to the fact that most of the literature experiments are generally less than a hundred trials.

The advantages of artificial intelligence and machine learning algorithms in manufacturing are vast [27] for researchers and practitioners. The adoption of these advanced technologies would enable fulfilling the demand of high-quality products in an efficient approach with reduced cost. Moreover, it would enable sustainable manufacturing such that the process can be simulated and the product quality can be predicted prior to conducting the manufacturing process, hence saving the material resources and time [27].

5. Conclusions

The prediction and modeling processes of machining parameters positively impact production in terms of saving time and resources. In this research, the Gaussian process regression (GPR) approach was utilized to model and predict cutting force in the turning process of AISI 4340 alloy steel. The accuracy of the model was evaluated against other benchmark methods such as SVM and ANN. The GPR outperformed these methods with a high degree of accuracy. The MAPE between experimental and predicted cutting force values was found to be 5.12%, and a superior coefficient of determination of $R^2 = 0.9843$ was also found. In addition, the GPR has the lowest computation time in terms of the training on the input dataset, where it was executed within 0.35087 s. The results suggest that the GPR could be utilized by process operators to predict cutting force parameters prior to the production process in order to save resources, and to design the experiment to yield the required production quality.

Author Contributions: Conceptualization, M.S.A. and A.M.A.; methodology, M.S.A. and A.M.A.; software, M.S.A. and A.M.A.; validation, M.S.A. and A.M.A.; formal analysis, M.S.A. and A.M.A.; investigation, M.S.A. and A.M.A.; resources, M.S.A. and A.M.A.; data curation, M.S.A. and A.M.A.; writing—original draft preparation, M.S.A. and A.M.A.; writing—review and editing, M.S.A. and A.M.A.; visualization, M.S.A. and A.M.A. All authors have read and agreed to the published version of the manuscript.

Funding: This research received no external funding.

Institutional Review Board Statement: Not applicable.

Informed Consent Statement: Not applicable.

Data Availability Statement: Not applicable.

Conflicts of Interest: The authors declare no conflict of interest.

Nomenclature

F_c	Resultant force (N)
F_f	Feed force (N)
F_t	Tangential force (N)
V	Cutting speed (m/min)
V_f	Feed rate (mm/rev)
d	Depth of cut (mm)

References

1. Zhang, G.; Guo, C. Modeling flank wear progression based on cutting force and energy prediction in turning process. *Procedia Manufact.* **2016**, *5*, 536–545. [CrossRef]
2. Suhil, H.; Ismail, N. Optimization of Cutting Parameters of Turning Operations by using Geometric Programming. *Am. J. Eng. Appl. Sci.* **2010**, *3*, 102–108.
3. Bera, T.C.; Manikandan, H.; Bansal, A.; Nema, D. A Method to Determine Cutting Force Coefficients in Turning Using Mechanistic Approach. *Int. J. Mater. Mech. Manuf.* **2018**, *6*, 99–103.
4. Korkmaz, M.E.; Günay, M. Finite Element Modelling of Cutting Forces and Power Consumption in Turning of AISI 420 Martensitic Stainless Steel. *Arab. J. Sci. Eng.* **2018**, *43*, 4863–4870. [CrossRef]
5. Thangarasu, S.K.; Shankar, S.; Tony Thomas, A.; Sridhar, G. Prediction of Cutting Force in Turning Process-an Ex-perimental Approach. *IOP Conf. Ser. Mater. Sci. Eng.* **2018**, *310*, 012119. [CrossRef]
6. Cica, D.; Sredanovic, B.; Lakic-Globocki, G.; Kramar, D. Modeling of the Cutting Forces in Turning Process Using Various Methods of Cooling and Lubricating: An Artificial Intelligence Approach. *Adv. Mech. Eng.* **2013**, *13*, 1–8. [CrossRef]
7. Altintas, Y. *Manufacturing Automation*, 2nd ed.; Cambridge University Press: Cambridge, UK, 2012.
8. Hanief, M.; Wani, M.; Charoo, M. Modeling and prediction of cutting forces during the turning of red brass (C23000) using ANN and regression analysis. *Eng. Sci. Technol. Int. J.* **2017**, *20*, 1220–1226. [CrossRef]
9. Zhang, G.; Guo, C. Modeling of Cutting Force Distribution on Tool Edge in Turning Process. *Procedia Manuf.* **2015**, *1*, 454–465. [CrossRef]
10. Fodor, G.; Sykora, H.T.; Bachrathy, D. Stochastic modeling of the cutting force in turning processes. *Int. J. Adv. Manuf. Technol.* **2020**, *111*, 213–226. [CrossRef]
11. Zerti, A.; Yallese, M.A.; Meddour, I.; Belhadi, S.; Haddad, A.; Mabrouki, T. Modeling and multi-objective optimization for minimizing surface roughness, cutting force, and power, and maximizing productivity for tempered stainless steel AISI 420 in turning operations. *Int. J. Adv. Manuf. Technol.* **2018**, *102*, 135–157. [CrossRef]
12. Tzotzis, A.; García-Hernández, C.; Huertas-Talón, J.-L.; Kyratsis, P. Influence of the Nose Radius on the Machining Forces Induced during AISI-4140 Hard Turning: A CAD-Based and 3D FEM Approach. *Micromachines* **2020**, *11*, 798. [CrossRef]
13. Patel, V.D.; Gandhi, A.H. Modeling of cutting forces considering progressive flank wear in finish turning of hardened AISI D2 steel with CBN tool. *Int. J. Adv. Manuf. Technol.* **2019**, *104*, 503–516. [CrossRef]
14. Sharma, V.; Kumar, P.; Misra, J.P. Cutting force predictive modelling of hard turning operation using fuzzy logic. *Mater. Today Proc.* **2020**, *26*, 740–744. [CrossRef]
15. Qiu, J. Modeling of cutting force coefficients in cylindrical turning process based on power measurement. *Int. J. Adv. Manuf. Technol.* **2018**, *99*, 1–11. [CrossRef]
16. Imani, L.; Henzaki, A.R.; Hamzeloo, R.; Davoodi, B. Modeling and optimizing of cutting force and surface roughness in milling process of Inconel 738 using hybrid ANN and GA. *Proc. Inst. Mech. Eng. Part B J. Eng. Manuf.* **2020**, *234*, 920–932. [CrossRef]
17. Chen, N.; Hao, B.; Guo, Y.; Li, L.; Khan, M.A.; He, N. Research on tool wear monitoring in drilling process based on APSO-LS-SVM approach. *Int. J. Adv. Manuf. Technol.* **2020**, *108*, 2091–2101. [CrossRef]
18. Pandiyan, V.; Caesarendra, W.; Tjahjowidodo, T.; Tan, H.H. In-process tool condition monitoring in compliant abrasive belt grinding process using support vector machine and genetic algorithm. *J. Manuf. Process.* **2018**, *31*, 199–213. [CrossRef]
19. Plaza, E.G.; López, P.J.N.; González, E.M.B. Multi-Sensor Data Fusion for Real-Time Surface Quality Control in Automated Machining Systems. *Sensors* **2018**, *18*, 4381. [CrossRef]
20. Garciaplaza, E.; Núñez, P.; Salgado, D.; Cambero, I.; Olivenza, J.H.; Sanz-Calcedo, J.G. Surface Finish Monitoring in Taper Turning CNC Using Artificial Neural Network and Multiple Regression Methods. *Procedia Eng.* **2013**, *63*, 599–607. [CrossRef]
21. Patole, P.; Kulkarni, V. Optimization of Process Parameters based on Surface Roughness and Cutting Force in MQL Turning of AISI 4340 using Nano Fluid. *Mater. Today Proc.* **2018**, *5*, 104–112. [CrossRef]
22. Rasmussen, C.E.; Williams, C.K.I. *Gaussian Processes for Machine Learning*; The MIT Press: New York, NY, USA, 2006.
23. Nguyen-Tuong, D.; Seeger, M.; Peters, J. Model Learning with Local Gaussian Process Regression. *Adv. Robot.* **2009**, *23*, 2015–2034. [CrossRef]
24. Grbić, R.; Kurtagić, D.; Slišković, D. Stream water temperature prediction based on Gaussian process regression. *Expert Syst. Appl.* **2013**, *40*, 7407–7414. [CrossRef]
25. Gopal, M. *Applied Machine Learning*; McGraw-Hill Education: New York, NY, USA, 2019.
26. Rasmussen, C.E. Gaussian processes in machine learning. In *Summer School on Machine Learning*; Springer: Berlin/Heidelberg, Germany, 2003; pp. 63–71.
27. Wuest, T.; Weimer, D.; Irgens, C.; Thoben, K.-D. Machine learning in manufacturing: Advantages, challenges, and applications. *Prod. Manuf. Res.* **2016**, *4*, 23–45. [CrossRef]